J Electroceram (2009) 23:468–473
DOI 10.1007/s10832-008-9497-z

Effect of heat treatment of sputter deposited ZnO films co-doped with H and Al

S. H. Lee · T. S. Lee · K. S. Lee · B. Cheong · Y. D. Kim · W. M. Kim

Received: 31 May 2007 / Accepted: 1 April 2008 / Published online: 26 April 2008
© Springer Science + Business Media, LLC 2008

Abstract ZnO films co-doped with H and Al (HAZO) were prepared by sputtering ZnO targets containing Al_2O_3 dcontent of 1 (HA_1ZO series) and 2 wt.% (HA_2ZO series) on Corning glass (Eagle 2000) at substrate temperature of 150 °C with Ar and H_2/Ar gas mixtures. The effects of hydrogen addition to Al-doped ZnO (AZO) films with different Al contents on the electrical, optical and structural properties of the as-grown films as well as the vacuum- and air-annealed films were examined. For the as-deposited films, the free carrier number in both series of HAZO films increased with increasing H_2 content in sputter gas. HA_2ZO film series prepared from target containing 2 wt.% Al_2O_3 showed better crystallinity and higher carrier concentration than HA_1ZO film series deposited using target containing 1 wt.% Al_2O_3. The crystallinity and the Hall mobility of HA_2ZO film series decreased with increasing H_2 content in sputter gas, while those of HA_1ZO film series showed a reversed behavior. Although HA_2ZO film series yielded lower resistivity than HA_1ZO film series due to higher carrier concentrations, the higher figure of merit (expressed as $1/\rho\alpha$, where ρ and α represents the resistivity and absorption coefficient, respectively) was observed for HA_1ZO film series because of substantially low absorption loss in these films. When annealed in air ambient, HA_1ZO film series showed much stronger stability than HA_2ZO film series. Vacuum-annealing resulted in drop of the carrier concentrations as well as large shrinkage in lattice constant, which indicated that the hydrogen dopants are in relatively volatile state and can be removed easily from the films upon annealing.

Keywords Hydrogen doping · ZnO · Transparent conducting oxide · Magnetron sputtering · Annealing

T. S. Lee · K. S. Lee · B. Cheong · W. M. Kim (✉)
Thin Film Materials Research Center,
Korea Institute of Science and Technology,
39-1, Hawolgok-dong, Sungbuk-gu,
Seoul 136-791, South Korea
e-mail: wmkim@kist.re.kr

S. H. Lee · Y. D. Kim
Division of Materials Science and Engineering,
Hanyang University,
17 Haengdang-dong, Seongdong-gu,
Seoul 133-791, South Korea

1 Introduction

Transparent conducting oxide (TCO) films have found a wide range of applications such as low-emissivity windows, electrochromic mirror and windows, defrosting windows, electromagnetic shielding, photovoltaic cells, and flat panel displays [1–3]. Sn doped In_2O_3 (ITO) films have been regarded as the representative of TCO due to its low resistivity and transparency obtained easily in production scale. But recent upsurge of indium price promoted researcher to search for an alternative TCO for ITO [4]. Impurity doped ZnO films are attractive TCO due to their low material cost, non-toxicity and stability under hydrogen plasma together with low resistivity and high visible transmission [5, 6].

First principle calculations have shown that, although hydrogen is usually observed as an amphoteric impurity in semiconducting or insulating materials, H^+ had lower energy than H^0 and H^- for any Fermi-level position when doped in ZnO, indicating that hydrogen in ZnO can act as shallow n-type donor [7, 8]. Along with these theoretical analyses, a number of experimental studies that back up the beneficial effect of hydrogen doping on pure ZnO and

metal-doped ZnO films can be found in the literature [9–18]. A few studies utilized post heat treatment method in hydrogen ambient to dope hydrogen into AZO films deposited by sputtering [9, 10], and into ZnO film grown by photo-MOCVD using a mercury-sensitized photo-CVD system [11–13]. Also, ZnO films [14, 15] and AZO films [16, 17] were deposited by sputtering in gas mixtures containing H_2. Doping of hydrogen into ZnO and AZO films revealed certain beneficial effects like improvement of electrical properties [9, 13, 15, 17] or enhanced stability in air [10, 12, 13, 16]. However, no study has been reported on the effect of hydrogen doping to AZO films with different Al contents and subsequent annealing effect on the electrical properties of the hydrogen doped AZO films. In this study, H-doped AZO films with different Al contents were prepared by radio frequency (rf) magnetron sputtering of ZnO targets with two different Al_2O_3 contents in H_2/Ar gas mixtures, and their electrical, optical and structural properties with respect to varying H and Al contents were examined. Also, an investigation on the changes in the electrical and structural properties upon annealing in air as well as in vacuum was made in order to elucidate the states of hydrogen incorporated into AZO films.

2 Experimental details

ZnO films co-doped with H and Al (HAZO) were prepared by rf magnetron sputtering of ZnO targets containing Al_2O_3 on Corning glass (Eagle 2000) at substrate temperature of 150 °C. ZnO targets with two different Al_2O_3 content of 1 and 2 wt.% were used. The hydrogen doping was made by introducing H_2 gas into the sputtering chamber while sputtering ZnO target containing Al_2O_3. The relative gas flow rate of H_2 and Ar was adjusted so that the volumetric gas flow ratio, $H_2/(H_2+Ar)$, in the sputter gas varied in the range from 0 to 8 vol.%. Each sample ID was denoted as H_aA_bZO, where subscript a represents per cent hydrogen volume flow ratio (i.e., $100H_2/(H_2+Ar)$) in sputter gas, and subscript b represents Al_2O_3 content in weight percent. The sample ID and corresponding per cent hydrogen volume flow ratio and thickness are listed in Table 1.

The base pressure in the chamber was kept below 5×10^{-5} Pa, and the sputtering deposition was carried out at a pressure of 0.16 Pa. The distance between the target and the substrate was 50 mm, and the RF power density was fixed at 2.5 W/cm^2. The substrate rotated at a constant speed of 12 rpm during sputtering. Annealing experiment was performed in a specially designed apparatus which can be pumped down to below 10^{-4} Pa and are equipped with multiple probes for the real-time measurement of the resistance change during the heating and cooling cycles. Annealing treatments of the as-prepared films were carried out in vacuum of 10^{-4} Pa or in atmosphere. The maximum temperature attained was around 310 and 300 °C for vacuum-annealing and air-annealing, respectively. Heating rate was 10 °C/min and natural cooling without forcing was applied.

Film thickness was measured by a surface profilometer after etching away part of the film with diluted HCl solution. The electrical resistivities, Hall mobilities, and carrier concentrations were determined from Hall-effect measurement using a Van der Pauw method. The structural analysis was carried out by an X-ray diffraction (XRD) measurement (Cu Kα wavelength=1.540562 Å, θ–2θ scan mode). The optical transmission and reflection spectra were obtained on a UV–visible spectrophotometer in wavelength ranges of 250–1,100 nm.

3 Results and discussion

Figure 1 summarizes the electrical resistivities, the Hall mobilities, and the carrier concentrations HA_1ZO and HA_2ZO film series plotted against H_2 content in sputter gas. For both series, the carrier concentration showed an increasing behavior with increasing H_2 content. The Hall mobility of HA_2ZO film series decreased monotonically with increasing H_2, resulting in only slight improvement of resistivity. H_4A_2ZO film gave the lowest resistivity of 2.94×10^{-4} Ω cm among all the prepared films. On the other

Table 1 List of sample IDs and the corresponding target composition and the hydrogen content in sputter gas.

$H_2/(Ar+H_2)$ (%)	HA_1ZO series		HA_2ZO series	
	$ZnO:Al_2O_3$ (1 wt.%)		$ZnO:Al_2O_3$ (2 wt.%)	
	Sample ID	Thickness (nm)	Sample ID	Thickness (nm)
0	H_0A_1ZO	275	H_0A_2ZO	280
2	H_2A_1ZO	388	H_2A_2ZO	268
4	H_4A_1ZO	382	H_4A_2ZO	260
6	H_6A_1ZO	374	H_6A_2ZO	275
8	H_8A_1ZO	292		

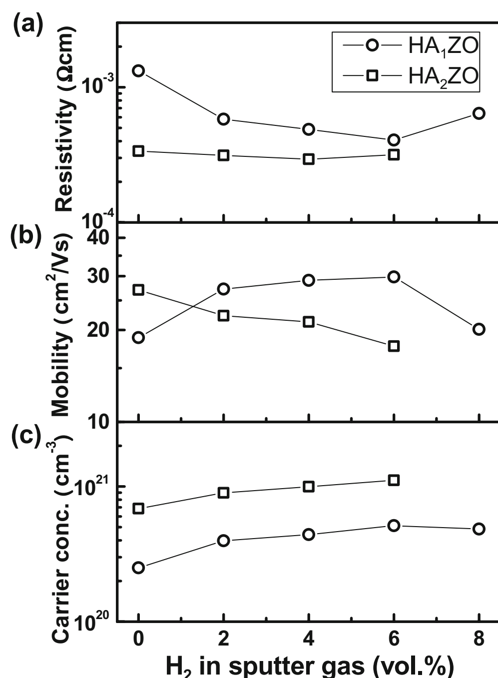

Fig. 1 Electrical properties of the as-deposited HAZO films, (**a**) resistivities, (**b**) Hall mobilities, and (**c**) carrier concentrations

hand, the Hall mobility of HA_1ZO film series increased for H_2 content up to 6 vol.%, then decreased. As a result, H_6A_1ZO film had the lowest resistivity of 4.07×10^{-4} Ω cm among HA_1ZO film series. It is well known that the electrical of TCO films depend on the film thickness. However, the variations in electrical properties and structural properties of doped ZnO films were shown to be pronounced at thickness below 200 nm [18, 19]. Since the thinnest film in this study was 260 nm, the effect of film thickness on the electrical properties would not be significant. Therefore, the variation of the electrical properties shown in Fig. 1 is ascribed largely to the effect of dopant concentration like Al and H. The increasing behavior of the free carriers and the Hall mobility in HA_1ZO film series with increasing H_2 content is almost the same as those observed in the work of Addonizio et al. [16]. However, the lowering of the Hall mobility observed for HA_2ZO film series is different from their result. This discrepancy is thought to stem from the difference in free carrier concentration range. Although Addonizio et al. used the AZO target containing the same Al_2O_3 content of 2 wt.% as HA_2ZO film series, their carrier concentration ranged from 4×10^{20} to 6×10^{20} cm^{-3}, which is rather comparable with the carrier concentration range obtained for HA_1ZO film series in this study.

The optical properties of the HAZO films were investigated in terms of optical absorption coefficient as shown in Fig. 2. Here, the optical absorption coefficient was evaluated by adopting relationship which is defined with corrections for reflection loss at the front surface of the sample, i.e. $\alpha = (1/d)\ln[(1-R)/T]$, where d, T and R are the film thickness, transmission and reflection, respectively [20]. The absorption spectra exhibit typical characteristics of TCO films, i.e., showing the minimum in visible wavelength region. This minimum absorption in visible region occurs due to the trade-off between the fundamental absorption mode located at ultraviolet (UV) region and the absorption mode in visible and near infra-red (IR) region. The absorption in visible and near IR region stems from various scattering centers such as free carriers, ionized impurities, phonon and neutral impurities, which increases gradually with increasing wavelength [21]. Three distinctive features observed from Fig. 2 are; (1) the relative overall level of the absorption coefficients for HA_1ZO film series is much lower than that for HA_2ZO film series, (2) the absorption coefficients in the long wavelength region of visible part and near infra-red part rise gradually with increasing H_2 content, and (3) the fundamental absorption edges are shifted toward higher energy side with increasing H_2. All these features reflect the free carrier behavior shown in Fig. 1. The inset in Fig. 2 shows the variations of transmittance averaged in visible range of 400–800 nm. For both series, small addition of hydrogen yielded enhancement of the average transmission. Although HA_2ZO films resulted in slight reduction of transmission at high H_2 content, HA_1ZO films maintained high transmission in all H_2 contents.

The figure of merit of TCO can be evaluated by taking the ratio of the conductivity to the absorption coefficient [22]. For H_4A_2ZO film, which had the lowest resistivity of 2.94×10^{-4} Ω cm, the calculated figure of merit using the absorption coefficient averaged in the range of 400–800 nm were 2.54 Ω^{-1}. On the other hand, the figure of merit estimated for H_6A_1ZO film with resistivity of 4.07×10^{-4} Ω

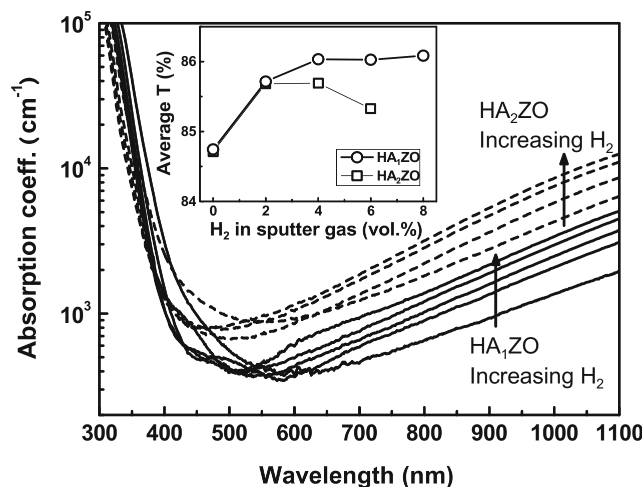

Fig. 2 Optical absorption coefficient spectra of as-deposited HAZO films. The *blue solid lines* and *black dashed lines* are for HA_1ZO and HA_2ZO film series, respectively. The *inset* shows variation of transmission averaged in wavelength ranges 400–800 nm

cm was 3.78 Ω^{-1}. This result indicates that the addition of hydrogen is more beneficiary for HA_1ZO films than for HA_2ZO films.

It has been reported that the electrical properties of AZO films were degraded upon annealing in air ambient [23]. In order to examine the effect of heat treatment of HAZO films, three samples from HA_1ZO and HA_2ZO series were selected and annealed in vacuum and air ambient. In Fig. 3, the changes in electrical resistivity, Hall mobility and free carrier concentration upon annealing are summarized. Some distinctive differences in the electrical behavior upon annealing between HA_1ZO and HA_2ZO series can be clearly seen. All the films underwent degradation of electrical properties upon air-annealing, the extent of degradation being different from sample to sample. The resistivity of air-annealed HA_2ZO film series increased substantially due to large reduction in the free carrier concentration as well as the Hall mobility. It is remarkable that the stability of H_2A_1ZO and H_6A_1ZO films in air ambient is much higher than H_2A_2ZO, H_6A_2ZO and even H_0A_1ZO films. Also, it is interesting to note that, except for H_0A_2ZO film, vacuum-annealing caused a substantial drop of carrier concentration. Especially, for H_6A_1ZO, H_2A_2ZO and H_6A_2ZO films, relatively large decrease in carrier concentration upon vacuum-annealing was observable. For vacuum-annealed H_2A_1ZO and H_6A_1ZO films, the decrease in free carrier number was accompanied with reduction of the Hall mobility. On the other hand, the Hall mobility of the vacuum-annealed H_2A_2ZO and H_6A_2ZO films increased slightly. Figure 4 shows the plot of the Hall mobility with respect to the free carrier concentration. The solid line drawn in the plot is showing the trace of the Hall mobilities of the as-deposited films. It is clear that the ionized impurity scattering came into playing a significant role in determining the Hall mobility in the case of HA_2ZO film series [24]. And this explains the reason for the decreased Hall mobility with increasing H_2 content in HA_2ZO film series. Also, for all the heat treated films except for H_0A_1ZO film, the lowering of the Hall mobility was accompanied with the drop of free carrier number. It is noticed that annealing of H_0A_1ZO film reduced the Hall mobility substantially despite slight increase in the carrier concentrations.

In Fig. 5, the change in transmission spectra of HA_2ZO film series upon annealing is shown. The transmission spectra of H_0A_2ZO film did not show a considerable change upon annealing. On the other hand, those of H_2A_2ZO and H_6A_2ZO films clearly show the red-shift of the fundamental absorption edge, the extent of shift being more pronounced in H_6A_2ZO film. Also, appreciable red-shift of the absorption edge can be seen even for the vacuum-annealed films. For all the annealed films, the transmittance in near IR range increased. These observations are in consistent with the changes in free carriers upon post heat treatment.

The structural properties of films were examined by XRD. For all the films, XRD profiles showed only strong peak from (002) plane, indicating a typical wurzite structure

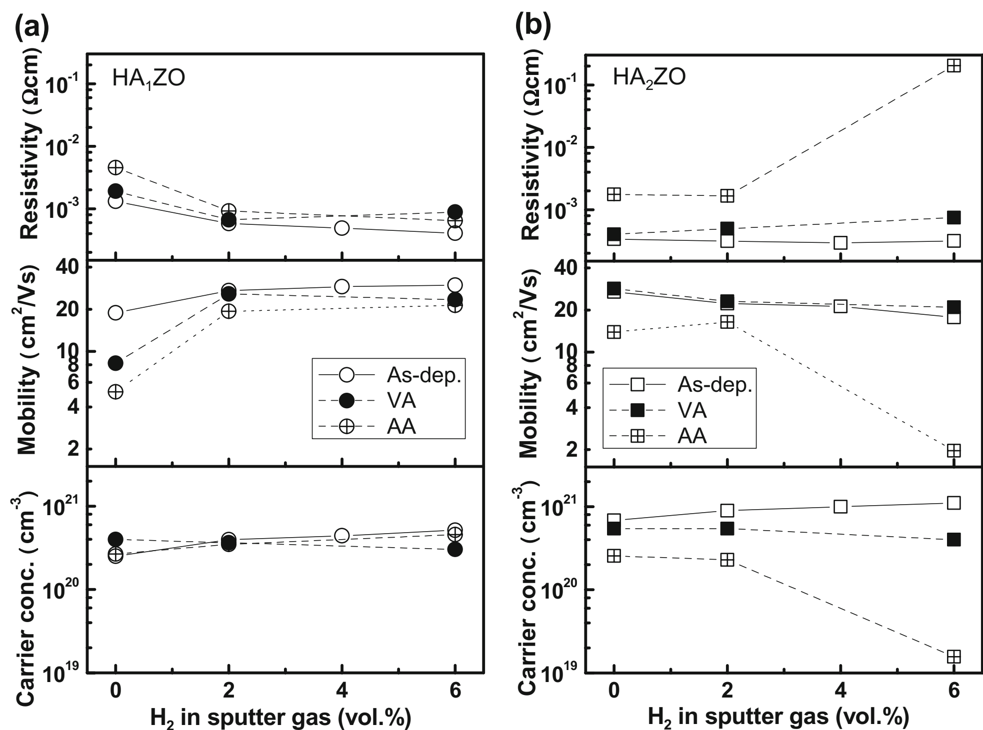

Fig. 3 Changes in electrical properties of (**a**) HA_1ZO film series, and (**b**) HA_2ZO film series upon air-annealing (*AA*) and vacuum-annealing (*VA*)

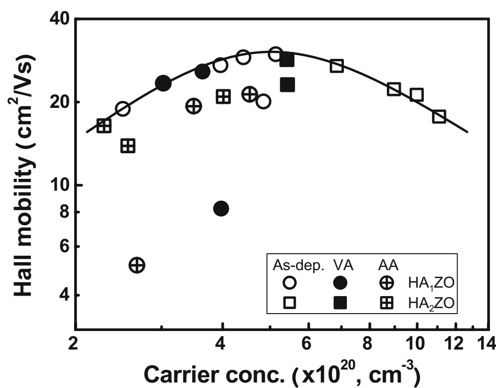

Fig. 4 Plot of the Hall mobility versus the carrier concentration. The *solid line* is drawn for an eye-guide to follow the trace of the as-deposited films

with (002) preferred orientation. Figure 6(a) shows the grain size estimated from the integral width of the (002) line according to the Scherrer formula by taking into account the instrumental peak broadening. Grain sizes of HA_1ZO film series were smaller than those of HA_2ZO films series. This is consistent with the observation that appropriate amount of dopant or impurity like Al acted as a mineralizer or surfactant which improves texturing of growing ZnO film [19]. Grain size increased with addition of H_2 content up to 4 vol.%. Further increase in H_2 resulted in reduction of grain size. The reduced grain size at high H_2 content is ascribed to; (1) the formation of the large number of nucleation sites at the initial stage of film growth, and (2) the inhibition of preferred crystalline growth due to passivation of growing film surface by either physically adsorbed hydrogen atoms or by O–H bonds formed on the growing film. The formation of O–H bonds might be probable because of the facts that the bond strength of O–H (4.4 eV) is larger than those of Zn–O (2.9 eV) and Zn–H (0.89 eV) [25], and that most of compound species like ZnO are dissociated into elemental ionic form of Zn^+ and O^- or O_2^- in rf discharge [19]. Annealing caused a slight increase in grain size, the extent of increase being larger for films without hydrogen.

Figure 6(b) shows the variation of (002) peak positions. For the as-deposited films, the (002) peak angle shifted gradually toward the lower angle side with increasing H_2, implying that the hydrogen incorporation caused an expansion of crystal lattice. This is in consistent with the results predicted by the first principle calculation, in which hydrogen incorporation into ZnO films would induce lattice expansion regardless of charge states and locations of the incorporated hydrogen [7]. The most striking feature noticeable from Fig. 6(b) is that the (002) peak angle of the annealed films increased very much, implying large shrinkage in *c*-axis lattice parameter. Combining the large shrinkage in *c*-axis lattice parameter with the decrease in the carrier concentrations observed for hydrogen added films upon vacuum-annealing indicates that hydrogen might have been removed from the films upon vacuum-annealing. In the case of air-annealing, the hydrogen removal and the adsorption of oxygen species at the grain

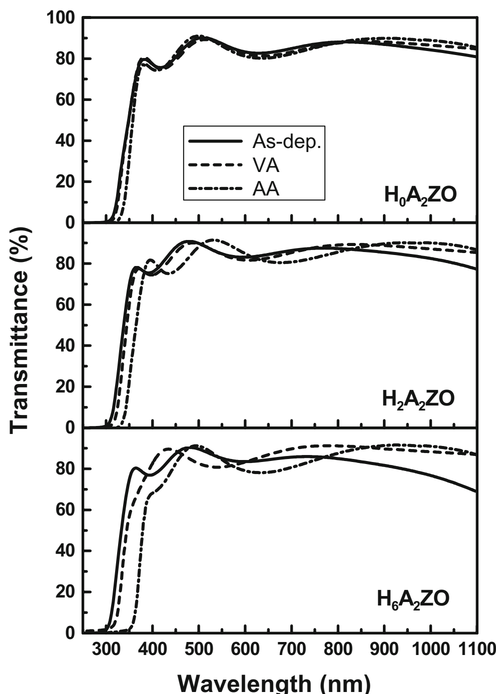

Fig. 5 Transmission spectra of the as-deposited and the annealed HA_2ZO film series

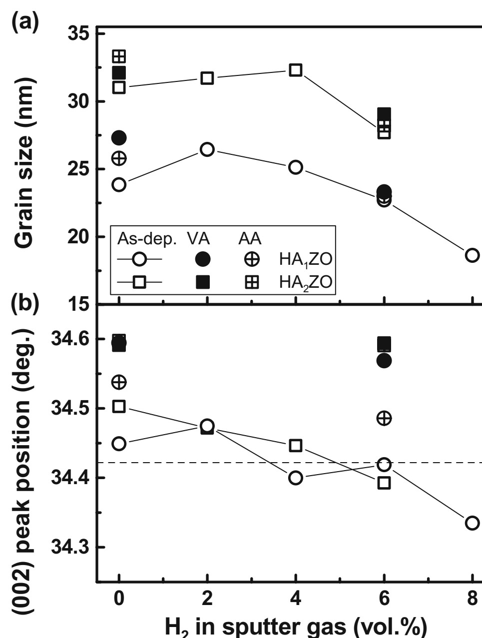

Fig. 6 Variations in (**a**) grain sizes, and (**b**) (002) peak positions of HAZO films

boundaries would take place simultaneously, which may explain the large drop of both the free carrier and the Hall mobility observed for air-annealed films with hydrogen. These observations lead to a perception that fairly large portion of hydrogen incorporated into the AZO films may be not only at the grain boundaries by filling in dangling bonds [10, 26] but in the locations with the lowest energy states as predicted by the first principle calculation [7]. Also, some of the hydrogen is thought to be combined states with oxygen vacancies, which seems probable considering that hydrogen in neutral oxygen vacancy was also suggested to form shallow donor [7, 13]. Since the binding energy of hydrogen and oxygen vacancy is small (0.8 eV) [7], this hydrogen can be removed easily by heat treatment.

4 Conclusions

In this work, ZnO films co-doped with H and Al were prepared on Corning glass by rf magnetron sputtering of ZnO target containing Al_2O_3 content of 1 (HA_1ZO series) and 2 wt.% (HA_2ZO series) on Corning glass (Eagle 2000) at substrate temperature of 150 °C with Ar and H_2/Ar gas mixtures. The electrical, optical and structural properties of the as-deposited as well as the air- and vacuum-annealed films were investigated. Addition of hydrogen resulted in increase of the carrier concentration for both film series. On the other hand, the Hall mobilities in HA_2ZO film series showed decreasing trend with increasing H_2 in sputter gas, while those in HA_1ZO film series increased. The decrease of the Hall mobility in HA_2ZO film series was caused by the increased scattering by ionized impurities. Although the HA_2ZO film series exhibited lower resistivity largely due to higher carrier concentration, it turned out that the addition of hydrogen was more beneficiary to HA_1ZO films than HA_2ZO films because of lower optical absorption combined with higher Hall mobility, leading to higher figure of merit in HA_1ZO film series. Both film series showed degradation in electrical properties upon air-annealing, but the degree of degradation is much larger for HA_2ZO film series. When annealed in vacuum, substantial reduction in the carrier concentration as well as in *c*-axis lattice parameter was observed in hydrogen added films. These observations led to an inference that fairly large portion of hydrogen may exist at the O–H bond center, at the grain boundaries, and at oxygen vacancies, all of which could be removed upon heat treatment at elevated temperature.

Acknowledgements This study was partially supported by a grant from the Fundamental R&D Program for Core Technology of Materials funded by the Ministry of Commerce, Industry and Energy, Republic of Korea.

References

1. K.L. Chopra, S. majors, K. Pandya, Thin Sold Films. **102**, 1 (1983)
2. A.L. Dawar, J.C. Joshi, J. Mater. Sci. **19**, 1 (1984)
3. R.G. Gordon, MRS Bull. **25**(8), 52 (2000)
4. J.F. Carlin Jr., *U.S. Geological Survey, Mineral Commodity Summaries*, Jan. (2006)
5. K. Ellmer, J. Phys. D: Appl. Phys. **34**, 3097 (2001)
6. T. Minami, MRS Bull. **25**(8), 38 (2000)
7. C.G. Van de Walle, Phys. Rev. Lett. **31**, 1012 (2000)
8. C.G. Van de Walle, J. Neugebauer, Nature **423**, 626 (2003)
9. B.-Y. Oh, M.-C. Jeong, D.-S. Kim, W. Lee, J.-M. Myoung, J. Crystal Growth, **281**, 475 (2005)
10. B.-Y. Oh, M.-C. Jeong, J.-M. Myoung, Appl. Surf. Sci. **253**, 7157 (2007)
11. S.J. Baik, J.H. Jang, C.H. Lee, W.Y. Cho, K.S. Lim, Appl. Phys. Lett. **70**(26), 3516 (1997)
12. S.Y. Myong, K.S. Lim, Appl. Phys. Lett. **82**(18), 3026 (2003)
13. M.S. Myong, S.I. Park, K.S. Lim, Thin Solid Films. **513**, 148 (2006)
14. Y-S. Kang, H.-Y. Kim, J.Y. Lee, J. Electrochem. Soc. **147**(12), 4625 (2000)
15. L.-Y. Chen, W.-H. Chen, J.-J. Wang, F.C.-N. Hong, Y.-K. Su, Appl. Phys. Lett. **85**, 5628 (2004)
16. M.L. Addonizio, A. Aantonaia, G. Cantele, C. Privato, Thin Solid Films. **349**, 93 (1999)
17. Y.M. Chung, C.S. Moon, W.S. Jung, J.G. Han, Thin Solid Films. **515**, 567 (2006)
18. T. Yamada, T. Nebiki, S. Kishimoto, H. Makino, K. Awai, T. Narusawa, T. Yamamoto, Superlattices and Microstructures **42**, 68 (2007)
19. R. Cebulla, W. Wendt, K. Ellmer, J. Appl. Phys. **83**, 1087 (1998)
20. K.S. Lee, T.S. Lee, I.H. Kim, B. Cheong, W.M. Kim, Integrated Ferroelectrics. **69**, 295 (2005)
21. I. Hamberg, C.G. Granqvist, J. Appl. Phys. **60**, R123 (1986)
22. S.A. Knickerbocker, A.K. Kulkami, J. Vac. Sci. Technol. A. **13**(3), 1048 (1995)
23. I.H. Kim, D.Y. Ku, J.H. Ko, D. Kim, K.S. Lee, J.-h. Jeong, T.S. Lee, B. Cheong, Y.-J. Baik, W.M. Kim, J. Electroceram. **17**, 241 (2006)
24. D.S. Ginley, C. Bright, MRS Bull. **25**(8), 15 (2000)
25. R.C. Weast, M.J. Astle (Eds.), *Handbook of Chemistry and Physics*, 61st Ed., (CRC, Boca Raton Fl, 1980–1981), pp. 225–226
26. S. Taketa, M. Fukawa, Thin Solid Films. **468**, 234 (2004)